



COB-2021-2338

PREDICTING VIBRATION ATTENUATION IN FINITE PERIODICALLY PINNED SUPPORTED BEAM STRUCTURES

Jean Paulo Carneiro Junior

jean.carneiro@unesp.br

Vinicius Germanos Cleante

State University of São Paulo – UNESP- School of Engineering, Ilha Solteira – Brazil

vinicius.cleante@unesp.br

Paulo José Paupitz Gonçalves

State University of São Paulo – UNESP- School of Engineering, Bauru – Brazil

paulo.paupitz@unesp.br

Michael John Brennan

State University of São Paulo – UNESP- School of Engineering, Ilha Solteira – Brazil

mjbrennan0@btinternet.com

Abstract. *One-dimensional waveguides are frequently found in structural engineering applications. They consist of long and thin elements, such that their properties can be well defined along with a single coordinate system. Examples of such systems include rods, beams, shafts and pipes. Often, these systems are assembled in periodic arrangements, where the whole system consists of a repetition of smaller units, known as cells. The periodicity can occur due to changes in the cell geometry, material properties, attachments, or boundary conditions. In this paper, wave propagation behaviour is investigated for the cases of simply supported beams, which can be modelled as a mono-coupled periodic system. Changes in the geometric properties are also induced to improve the so-called attenuation bands, which are frequency ranges where waves are not cancelled, but severely reduced. Because bending waves are dispersive and dependent on the cross-section shape, the geometric changes are made so that the ratio of the second moment of area and cross-section area between two different beams remain fixed. The analysis consists of modelling a single cell using the concept of displacement transmissibility, which is a measurable quantity. Approximate analytical expressions are derived to predict the bandwidths of the attenuation bands and the maximum attenuation for a single cell. These expressions can be used to estimate the attenuation for a system consisting of N periodic cells.*

Keywords: *Periodic structures, angular transmissibility, transfer matrix, pinned stepped beam.*

1. INTRODUCTION

One-dimensional systems, such as beams and rods are used in many engineering applications. In some cases, they have an abrupt change in cross-section. This paper concerns the study of a stepped beam in the formation of a periodic structure. The vibrations of stepped beams have been studied for many years. Initial research was aimed at determining exact and numerical solutions to predict their dynamic behaviour, applying different tools during the process (Jang and Bert 1989a; Taleb and Suppiger 1961).

Studies concerning the exact solutions and natural frequencies of stepped beams conducted by (Jang and Bert 1989b), formed an important basis in the development of models for a supported stepped beam model. Since then, more complex systems have been considered, such as multiple steps and property variation (Fazeli et al. 2021; Lin and Ng 2017; Mao 2011). Other approaches have focused on analytical methods and the evaluation of mode shapes. Sato (1983) developed an analytical approach combining the Transfer Matrix Method (TMM) and the Finite Element Method (FEM), demonstrating that simple beam theory leads to a noticeable error for specific groove geometries, thus requiring additional approaches. Analytical solutions for stepped beam receptance were determined by (Koplow, Bhattacharyya, and Mann 2006), which were validated by experimental tests. The transfer matrix approach groups the force and displacement at particular points of the structure into a state-vector. It is interchangeable with the receptance and dynamic stiffness matrices (Gonzalez-Bueno 2019). Since the approach was proposed, its main advantages have been evident in the mathematical simplicity, reduction of computational effort, and the direct relationship with easily measurable quantities (Hull and Cray 2014).

Recent work also aimed to simplify the analyses, such as the study conducted by (Zheng and Ji 2011), which proposes an equivalent representation of a multistep beam to significantly simplify the calculation of design parameters. Alternative ways to simplify analytical expressions and determine natural frequencies and mode shapes of a beam subjected to

different boundary conditions and combinations of lumped parameters was discussed by (Gonçalves et al. 2018; Gonçalves et al. 2019).

A periodic structure made up of stepped beams can be analysed using Floquet theory. In infinite periodic structures there are frequency ranges in which waves can or cannot propagate, and these are known as passbands and stopbands respectively. However, in practical cases, structures are finite, and consequently, other effects are important, such as the structural boundaries. In this paper a periodic structure that is comprised of stepped beams and periodic supports is studied to determine the dominant effects in the vibration transmission through the structure. It is assumed that the beams can be modelled using Euler-Bernoulli beam theory. To achieve this objective, the transfer matrix approach is used and approximate analytical expressions are derived to predict the frequency ranges of the attenuation bands and the maximum attenuation for a single cell or a structure comprising multiple cells.

2. PROBLEM STATEMENT

Consider the bending vibration of the finite beam, shown in Figure 1a. It has transverse forces, bending moments, transverse and rotational displacements, represented respectively by F , M , W and, Θ ; the subscripts indicate the left (L) and right (R) ends of the structure. Replicating this beam section N times, produces a system in which displacements and rotations at the ends of the cell couple with displacement and rotations of the connecting cells. It is thus not a mono-coupled system as in a periodic structure comprising of only of rods. Because of this, the mathematical description of the structure is a cumbersome. One way to maintain the simplicity of a mono-coupled system is to place pins at the ends of each beam in the periodic array. This is shown for a single beam element in Figure 1b, and schematically for a complete structure with N cells in Figure 2. In addition to simplifying the problem, this condition facilitates the application of the methodology proposed by (Gonçalves et al. 2021) to the problem and makes comparisons with the effects observed for a periodic structure comprised of rods described in (Carneiro Jr et al. 2021).

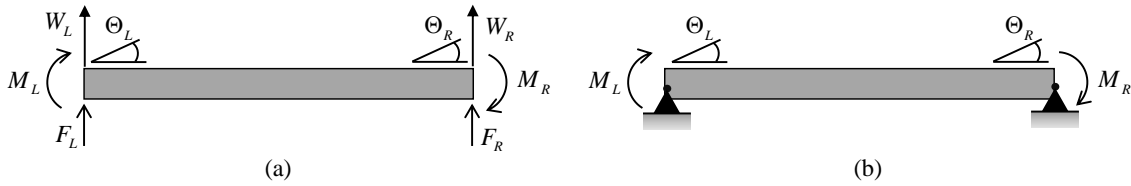


Figure 1. General one-dimensional single-cell beams elements under different boundary conditions at ends.
 (a) Free-free. (b) Pinned supports.

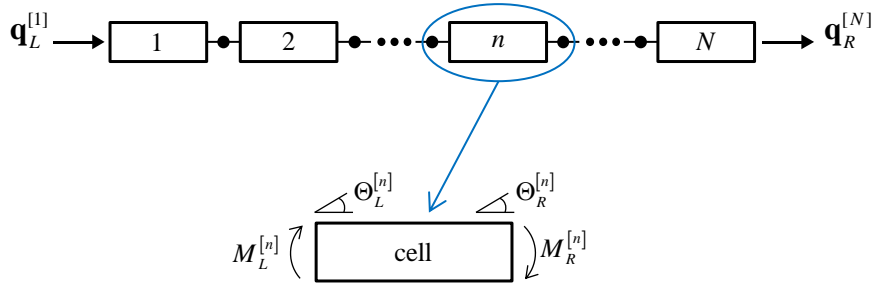


Figure 2. General mono-coupled structure composed of N one-dimensional cells, subjected to moments excitations, with emphasis on the n -th cell.

The relationship between the force and displacement at the right-hand end of the structure in Figure 2 to the force and displacement at the left-hand end is given by

$$\mathbf{q}_R^{[N]} = \mathbf{T}_g \mathbf{q}_L^{[1]}, \quad (1)$$

where $\mathbf{q}_R = \{M_R, \Theta_R\}^T$, $\mathbf{q}_L = \{M_L, \Theta_L\}^T$ and \mathbf{T}_g is the global transfer matrix.

There are alternative ways of determining the global transfer matrix. One way is to raise the N -th power the transfer matrix of a single cell, i.e., by,

$$\mathbf{T}_g = \mathbf{T}_{cell}^N = \begin{bmatrix} T_{11} & T_{12} \\ T_{21} & T_{22} \end{bmatrix}^N. \quad (2)$$

The terms in the matrix can be determined using the Cayley-Hamilton theorem, (Gonçalves et al. 2021), and are given by

$$\mathbf{T}_g = \begin{bmatrix} \cosh(N\mu) + (T_{11} - T_{22}) \frac{\sinh(N\mu)}{2\sinh(\mu)} & \frac{T_{12} \sinh(N\mu)}{\sinh(\mu)} \\ \frac{T_{21} \sinh(N\mu)}{\sinh(\mu)} & \cosh(N\mu) + (T_{11} - T_{22}) \frac{\sinh(N\mu)}{2\sinh(\mu)} \end{bmatrix}, \quad (3)$$

where $\mu = \text{acosh}\left(\frac{T_{11} + T_{22}}{2}\right)$. The propagation constant μ is related to the eigenvalues of the transfer matrix for a single cell \mathbf{T}_{cell} , and provides important information about the behaviour of the structure. If μ is purely imaginary, there is no attenuation, that is, there is a pass band. However, if μ is real, there is attenuation, that is, there is a stop band. Additionally, it is important to note that the elements (1,1), (1,2), (2,1) and (2,2) of the transfer matrices correspond respectively to the moment transmissibility, transfer dynamic stiffness, transfer receptance and the rotational displacement transmissibility. The present work focuses on the study of the displacement transmissibility.

The transmissibility is given by $\frac{\Theta_R^{[N]}}{\Theta_L^{[1]}} \Big|_{M_R=0}$, which is the reciprocal of element 2,2 in the matrix \mathbf{T}_g^{-1} . From Equation

(3) the rotational displacement transmissibility for the complete structure with N cells is given by

$$\frac{\Theta_R^{[N]}}{\Theta_L^{[1]}} \Big|_{M_R=0} = \frac{2\sinh(\mu)}{2\sinh(\mu)\cosh(N\mu) + (T_{11} - T_{22})\sinh(N\mu)}. \quad (4)$$

Note that the transmissibility for the complete structure is expressed in terms of the properties for a single cell and the number of cells N . Equation (4) is considerably simplified if the cell is symmetric because, in this case, $T_{11} = T_{22}$. Part of the work presented in this paper, discusses the symmetry and asymmetry relationships based on the cells shown in Figure 3.

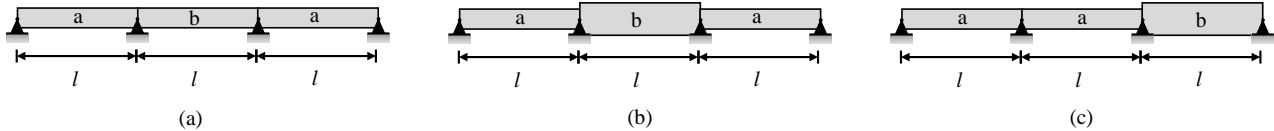


Figure 3. Single-cell elements with in different configurations. (a) homogeneous symmetric; (b) discontinuous symmetric and (c) asymmetric cell.

3. DISPLACEMENT TRANSMISSIBILITY OF SYMMETRIC AND ASYMMETRIC CELLS

3.1 Homogeneous cell

The only discontinuity for the homogenous cell structure shown in Fig. 3(a) is due to the pinned supports. The arrangement of the pins supports followed the logical order of construction in practical cases. The cell sections, or sub-cell, labelled either a or b, have the same geometric and material properties, thus the Young's modulus $E_a = E_b$, the density $\rho_a = \rho_b$, the second moment of area $I_a = I_b$, the cross-section area $S_a = S_b$, and the section length $l_a = l_b = l$.

The transfer matrix for a generic pinned supported beam i presented in Figure 1(b), is given by

$$\mathbf{T}_i = \begin{bmatrix} \frac{\cos(k_i l) \sinh(k_i l) - \cosh(k_i l) \sin(k_i l)}{\sinh(k_i l) - \sin(k_i l)} & -\frac{2E_i I_i k_i \sin(k_i l) \sinh(k_i l)}{\sinh(k_i l) - \sin(k_i l)} \\ \frac{\cos(k_i l) \cosh(k_i l) - 1}{E_i I_i k_i (\sinh(k_i l) - \sin(k_i l))} & \frac{\cos(k_i l) \sinh(k_i l) - \cosh(k_i l) \sin(k_i l)}{\sinh(k_i l) - \sin(k_i l)} \end{bmatrix}, \quad (5)$$

where, $k_i = \sqrt{\omega}(\rho_i S_i / E_i I_i)^{\frac{1}{4}}$ is the beam wavenumber. Equation (5) is used as a basis for assembling the cells of Figure 3, so that, the cell transfer matrix can be obtained by replacing the properties of each sub-cell and noting that $\mathbf{T}_{cell}^{[Homo]} = \mathbf{T}_a \mathbf{T}_b \mathbf{T}_a$, or $\mathbf{T}_{cell}^{[Homo]} = \mathbf{T}_a^3$, since the length of a is the same as the length of b.

The hyperbolic functions in Eq. (5) represent the evanescent waves on the beam at the boundaries which become increasingly localized as frequency increases. An approximation is applied to the transmissibility of a single cell can be applied by considering that $\sinh(k_i l) \approx \cosh(k_i l)$, when $k_i l \gg 1$ as discussed by (Gonçalves et al. 2007; Gonçalves et al. 2018). Note that $k_i l$ can be conveniently written as a function of non-dimensional length and normalized in terms of sub-cell a properties, so $k_a l = 2\pi \frac{l}{\lambda_a}$, where λ_a is the wavelength. For the cases studied the approximation turns out to be valid when $\lambda_a < 2l$, which is discussed later. Applying these considerations, the angular displacement transmissibility for one single homogeneous cell, is found to be

$$|T|^{[Homo]} \approx \frac{1}{\sqrt{2} \sin(2\pi l/\lambda - \pi/4) (4 \sin(4\pi l/\lambda) - 1)}, \text{ for } \frac{l}{\lambda_a} > \frac{1}{2}. \quad (6)$$

3.2 Symmetric and asymmetric discontinuous cell

As well as creating periodicity by applying pinned supports, beams with different cross-sections can also be used as shown in Figs. 3(b) and (c). To keep the wave-speeds the same in each beam section, the wavenumber in section a should be the same as in section b, so that $k_a = k_b$. For beams made from the same material, this means that $\frac{S_a}{I_a} = \frac{S_b}{I_b}$, resulting in hollow beams. Similar to the procedure applied for the homogeneous cell in Fig. 3(a), the transfer matrices for the cells in Figure 3(b) and Figure 3(c) are respectively given by

$$\mathbf{T}_{cell}^{[Sym]} = \mathbf{T}_a \mathbf{T}_b \mathbf{T}_a \quad (7)$$

and

$$\mathbf{T}_{cell}^{[Asym]} = \mathbf{T}_b \mathbf{T}_a \mathbf{T}_a. \quad (8)$$

The transfer matrices of each section can be rewritten by dividing Θ_L and multiplying Θ_R by $E_a I_a k_a$. This procedure results in a dimensionless cell transfer matrix with a parameter that relates the second moment of area of section a and b, that is the ratio of moments of area, given by $\beta = \frac{\text{sub-cell b second moment of area}}{\text{sub-cell a second moment of area}} = \frac{I_b}{I_a}$. Note that if $\beta > 1$, the corresponding cell is similar to the shown in Figure 3(c). However, if $\beta < 1$, the corresponding structure is the opposite of the representation in Figure 3, i.e., sub-cell a has a greater second moment of area than sub-cell b.

As in the previous section, the high-frequency approximation is applied and the angular displacement transmissibility for a single symmetric cell is determined, as

$$|T|^{[Sym]} \approx \frac{1}{\sqrt{2} \sin(2\pi l/\lambda - \pi/4) [(\beta + 3) \sin(4\pi l/\lambda) - 1]}, \text{ for } \frac{l}{\lambda_a} > \frac{1}{2}, \quad (9)$$

and for a single asymmetric cell

$$|T|^{[Asym]} \approx \frac{1}{\sqrt{2} \sin(2\pi l/\lambda - \pi/4) [2(\beta + 1) \sin(4\pi l/\lambda) - 1]}, \text{ for } \frac{l}{\lambda_a} > \frac{1}{2}. \quad (10)$$

It can be seen from Equations (9) and (10) that if $\beta = 1$, the expressions reduce to Eq. (6). These approximate analytical expressions and the numerical results are presented in Figure 4 as a function of l/λ . To limit the response at the resonance frequencies, a loss factor of $\eta = 0.01$ is assumed to add some damping to the structure. Note that the approximation, i.e., Eqs. (6), (9) and (10) can be used to describe the stop band of interest. It is observed that regardless

of the symmetry of the cell, the lower and upper bounding frequencies, demarcated by the red dash line, are constant and equal to $\frac{l}{\lambda}\Big|_{\text{lower}} = \frac{3}{4}$ and $\frac{l}{\lambda}\Big|_{\text{upper}} = 1$, respectively. In addition, the minimum transmissibility frequency, highlighted by the black dash-dot line, is also constant and equal to $\frac{l}{\lambda}\Big|_{\text{min}} = \frac{7}{8}$. This analysis facilitates the prediction of the stop band and allows simplification of the complete expression.

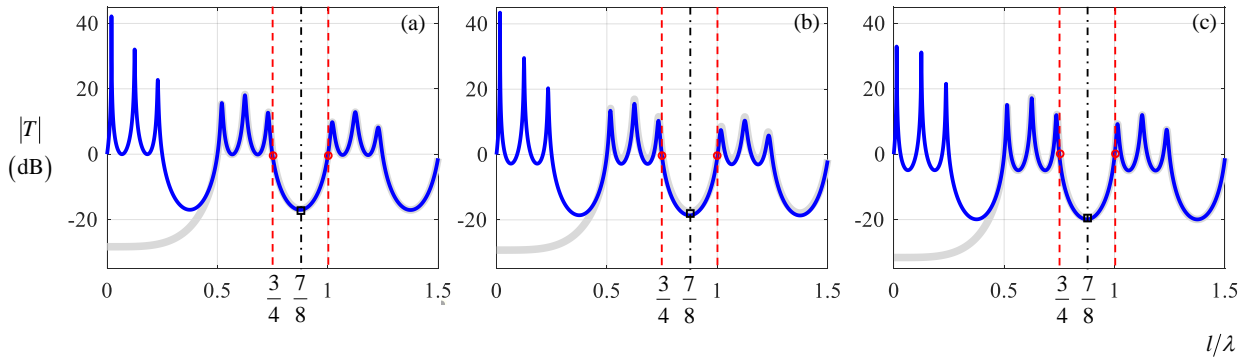


Figure 4. Displacement transmissibility of a periodic supported beam comprising: (a) homogeneous symmetric single cell; (b) symmetric single cell with $\beta = 2$ and (c) asymmetric single cell with $\beta = 2$. The thick gray line corresponds to numerical expression results and thin blue line corresponds to analytical approximation expression.

The transmissibility for a symmetric structure with N cells can be determined from Eq. (4). Due to the cell symmetry Eq. (4) simply becomes

$$\frac{\Theta_R^{[N]}}{\Theta_L^{[1]}} \Big|^{[\text{Sym}]} = \frac{1}{\cosh(N\mu)}. \quad (11)$$

Since $\text{acosh}(x) = \ln(x + \sqrt{x^2 - 1})$, this expression can be written as

$$\frac{\Theta_R^{[N]}}{\Theta_L^{[1]}} \Big|^{[\text{Sym}]} = \frac{2}{\left(\frac{1}{T} + \sqrt{\frac{1}{T^2} - 1}\right)^N + \left(\frac{1}{T} + \sqrt{\frac{1}{T^2} - 1}\right)^{-N}}. \quad (12)$$

Therefore, the transmissibility of the complete symmetric structure can be determined from the transmissibility of a single cell T . Additionally, it appears that the minimum transmissibility of N cells for the asymmetric structure is not easily determined, as Eq. (4) cannot be easily simplified.

4. DISCUSSION

Figure 5 shows the transmissibilities for different values of β . It is observed that for symmetric cell β or $1/\beta$ results in the same transmissibility. However, this behaviour is not valid for asymmetric cells, demonstrating that cell orientation is important in terms of attenuation. It is also observed that an asymmetrical cell results in greater vibration attenuation when compared to symmetrical structures. These effects were observed and discussed by (Carneiro Jr et al. 2021), in the evaluation of periodic rods. This is because the point receptance is greater for a thinner cell section than for a thicker cell section. Hence attenuation occurs from left to right for the asymmetric cell shown in Figure 3(c), but there is amplification from left to right for the opposite orientation.

Regarding the boundary frequencies, the results presented in Figs. (4) and (5) allow us to infer that although β influences the maximum attenuation, this parameter does not influence the boundary frequencies. This is because these frequencies are controlled by boundary conditions at the ends and correspond to the pinned-pinned and fixed-fixed natural frequencies of the single cell, and alternate their positions as $\beta > 1$ or $\beta < 1$ for symmetric structures. A similar result was described by (Mead 1975), in the study of mono-coupled systems.

Note that it is possible to substitute $\left. \frac{l}{\lambda} \right|_{\min} = \frac{7}{8}$ in Eqs. (6) and (9) to determine the minimum transmissibility for a single cell. For example, the homogeneous cell the process results in $|T|_{\min}^{[\text{Homo}]} = \frac{1}{5\sqrt{2}}$, which corresponds to approximately -17 dB. To determine the minimum transmissibility for N cells, this result is replaced in Eq. (12). The result of this procedure can be conveniently rewritten in terms of maximum attenuation, A in dB and expressed by

$$A \approx 20 \log_{10} (7 + 5\sqrt{2}) N - 6. \quad (13)$$

Equation (13) demonstrates that each additional cell in the structure increases approximately 23 dB in attenuation, which in engineering terms is extremely significant. Figure 6 shows the comparison of the transmissibility of one, two, and three symmetrical and asymmetrical cells. A loss factor of 0.01 was assumed and the frequency range is limited to the stop band of interest. It is observed that the increase in cells results in a considerable reduction in the transmitted vibration. However, there is no significant difference in the minimum transmissibility between the different cell arrangements.

This analysis demonstrates that transmissibility is mainly controlled by pinned support distribution. Therefore, in practical cases, the simple correct distribution of the supports allows the structure to perform high attenuation between an excitation device and the receiver at the ends. Table 1 summarizes the expressions developed in this work. The boundary frequencies and minimum transmissibility are also tabulated.

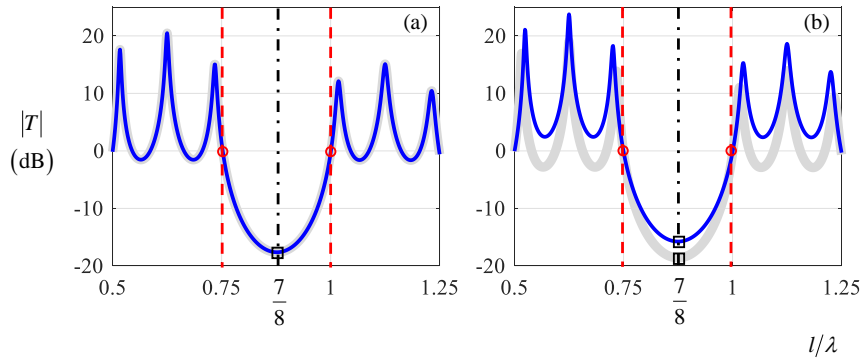


Figure 5. Displacement transmissibility of a periodic supported beam for: $\beta = 1.25$, thick gray line and $\beta = 0.8$ thin blue line. (a) symmetric single cell (Figure 3(b)) and (b) asymmetric single cell (Figure 3(c)).

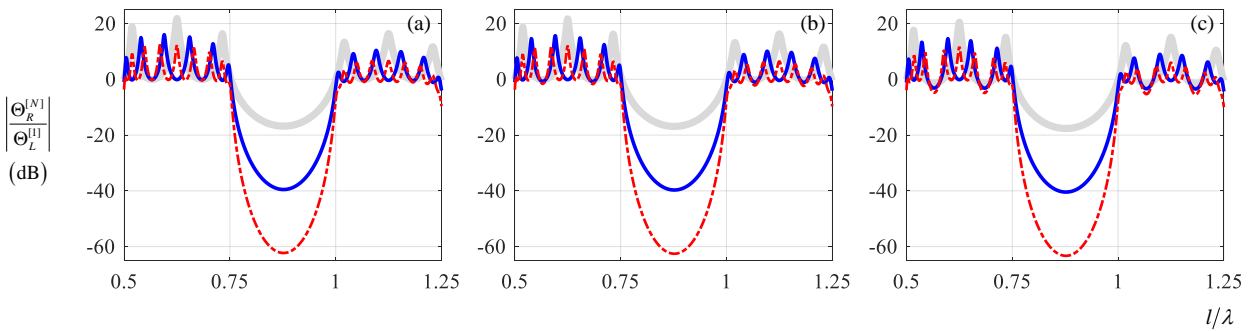


Figure 6. Displacement transmissibility for $N = 1$, thick gray line; $N = 2$, thin blue line and $N = 3$, red dash-dot line. (a) Homogeneous cell, (b) discontinuous symmetric cell with $\beta = 1.25$ and (c) asymmetric cell with $\beta = 1.25$.

Table 1. Approximate expressions and features for predicting minimum transmissibility for symmetrical and asymmetric cells.

Structure	Approximation $ T $		Bounding frequency		Minimum transmissibility	
			$\frac{l}{\lambda} _{\text{lower}}$	$\frac{l}{\lambda} _{\text{upper}}$	$\frac{l}{\lambda} _{\text{min}}$	$ T _{\text{min}}$
Figure 3(a)	$\frac{1}{\sqrt{2} \sin(2\pi l/\lambda - \pi/4)(4 \sin(4\pi l/\lambda) - 1)}$	$\beta = 1$				$\frac{1}{5\sqrt{2}}$
Figure 3(b)	$\frac{1}{\sqrt{2} \sin(2\pi l/\lambda - \pi/4)[(\beta + 3) \sin(4\pi l/\lambda) - 1]}$	$\beta > 0$	$\frac{3}{4}$	1	$\frac{7}{8}$	$\frac{1}{\sqrt{2}(\beta + 4)}$
Figure 3(c)	$\frac{1}{\sqrt{2} \sin(2\pi l/\lambda - \pi/4)[2(\beta + 1) \sin(4\pi l/\lambda) - 1]}$	$\beta > 1$				$\frac{1}{\sqrt{2}(2\beta + 3)}$

5. CONCLUSIONS

This paper has described an investigation into the vibration transmission through a periodic structure comprised of beam elements. Two types of discontinuity were introduced into the structure. One involved periodic pinned supports and the other involved periodic step changes in the cross-section of the beam. The effects of both of these discontinuities on the vibration transmission through a structure with N cells were investigated. To ensure that the system was relatively simple to analyse, the wave speed was kept constant in all the sub-cells by arranging the geometry in a specific way. Both symmetric and asymmetric cells were evaluated, and expressions for the bounding frequencies of a low frequency stop-band and the minimum transmissibility within this stop band were derived. It was found that the dominant periodic effect in terms of vibration attenuation was the pinned supports rather than the step changes in cross-section, and because the structure was effectively mono-coupled, the stopband boundary frequencies correspond to the natural frequencies for pinned-pinned and fixed-fixed boundary conditions for a single cell. Furthermore, these frequencies are independent of the number of cells in the periodic structure.

6. ACKNOWLEDGEMENTS

The authors would like to acknowledge the financial support of the São Paulo Research Foundation (FAPESP), grant numbers 2018/ 15894-0, 2019/19335-9 and 2020/00659-6.

7. REFERENCES

- Carneiro Jr, J. P., Brennan, M. J., Gonçalves, P. J. P., Cleante, V. G., Bueno, D. D. and Santos, R. B. 2021. "On the Attenuation of Vibration Using a Finite Periodic Array of Rods Comprised of Either Symmetrical or Asymmetrical Cells." *Journal of Sound and Vibration*. doi: 10.1016/j.jsv.2021.116217.
- Fazeli, S., Stokes-Griffin, C., Gilbert, J. and Compston, P. 2021. "An Analytical Solution for the Vibrational Response of Stepped Smart Cross-Ply Laminated Composite Beams with Experimental Validation." *Composite Structures* 266. doi: 10.1016/j.compstruct.2021.113823.
- Gonçalves, P. J. P., Brennan, M. J., and Cleante, V. G. 2021. "Predicting the Stop-Band Behaviour of Finite Mono-Coupled Periodic Structures from the Transmissibility of a Single Element." *Mechanical Systems and Signal Processing* 154. doi: 10.1016/j.ymsp.2020.107512.
- Gonçalves, P. J. P., Brennan, M. J., and Elliott, S. J. 2007. "Numerical Evaluation of High-Order Modes of Vibration in Uniform Euler-Bernoulli Beams." *Journal of Sound and Vibration* 301(3-5). doi: 10.1016/j.jsv.2006.10.012.
- Gonçalves, P. J. P., Brennan, M. J., Peplow, A. and Tang, B. 2019. "Calculation of the Natural Frequencies and Mode Shapes of a Euler-Bernoulli Beam Which Has Any Combination of Linear Boundary Conditions." *Journal of Vibration and Control* 25(18). doi: 10.1177/1077546319857336.
- Gonçalves, P. J. P., Peplow, A., and Brennan, M. J. 2018. "Exact Expressions for Numerical Evaluation of High Order Modes of Vibration in Uniform Euler-Bernoulli Beams." *Applied Acoustics* 141. doi: 10.1016/j.apacoust.2018.05.014.
- Gonsalez-Bueno, C. G. 2019. "An Investigation into the Way in Which Longitudinal and Flexural Waves Interact with Corrosion-like Damage." State University of São Paulo (UNESP). School of Engineering.
- Hull, A. J., and Benjamin A. C.. 2014. "Response of Infinite Length Rods and Beams with Periodically Varying Area." *Journal of Sound and Vibration* 333(20):4960-76. doi: 10.1016/j.jsv.2014.04.041.
- Jang, S. K., and Bert, C. W. 1989a. "Free Vibration of Stepped Beams: Exact and Numerical Solutions." *Journal of*

- Sound and Vibration* 130(2). doi: 10.1016/0022-460X(89)90561-0.
- Jang, S. K., and Bert, C. W. 1989b. "Free Vibration of Stepped Beams: Higher Mode Frequencies and Effects of Steps on Frequency." *Journal of Sound and Vibration* 132(1). doi: 10.1016/0022-460X(89)90882-1.
- Koplow, M. A., Bhattacharyya, A. and Mann, B. P. 2006. "Closed Form Solutions for the Dynamic Response of Euler-Bernoulli Beams with Step Changes in Cross Section." *Journal of Sound and Vibration* 295(1-2). doi: 10.1016/j.jsv.2006.01.008.
- Lin, R. M., and Ng, T. Y. 2017. "Exact Vibration Modes of Multiple-Stepped Beams with Arbitrary Steps and Supports Using Elemental Impedance Method." *Engineering Structures* 152. doi: 10.1016/j.engstruct.2017.07.095.
- Mao, Q. 2011. "Free Vibration Analysis of Multiple-Stepped Beams by Using Adomian Decomposition Method." *Mathematical and Computer Modelling* 54(1-2). doi: 10.1016/j.mcm.2011.03.019.
- Mead, D. J. 1975. "Wave Propagation and Natural Modes in Periodic Systems: I. Mono-Coupled Systems." *Journal of Sound and Vibration* 40(1):1-18. doi: 10.1016/S0022-460X(75)80227-6.
- Sato, H. 1983. "Free Vibration of Beams with Abrupt Changes of Cross-Section." *Journal of Sound and Vibration* 89(1). doi: 10.1016/0022-460X(83)90910-0.
- Taleb, N. J., and Suppiger, E. W. 1961. "Vibration of Stepped Beams." *Journal of the Aerospace Sciences* 28(4). doi: 10.2514/8.8962.
- Zheng, T. and Ji, T. 2011. "Equivalent Representations of Beams with Periodically Variable Cross-Sections." *Engineering Structures* 33(3). doi: 10.1016/j.engstruct.2010.11.007.

8. RESPONSIBILITY NOTICE

The author(s) is (are) the only responsible for the printed material included in this paper.